Powder Technology 412 (2022) 118025

Contents lists available at ScienceDirect

Powder Technology

journal homepage: www.journals.elsevier.com/powder-technology

Optimization of briquetting technology of fine-grained metallurgical materials based on statistical models of compressibility

Alexander Khudyakov [a], Sergii Vashchenko [a], Kostiantyn Baiul [a], Yurii Semenov [a], Pavlo Krot [b,*]

[a] Iron and Steel Institute of Z.I. Nekrasov, NAS of Ukraine, Dnipro, Ukraine
[b] Faculty of Geoengineering, Mining and Geology, Wroclaw University of Science and Technology, Wroclaw, Poland

HIGHLIGHTS

- The cold-bonded briquetting is an eco-friendly technology of fine-grained metallurgical charges agglomeration.
- A new indicator for the fine fractions compression evaluation is developed based on the original equation.
- Statistical models of compressibility are obtained using a three-level design of experiment plans.
- Models are optimized by response surface analysis and the method of indefinite Lagrange multipliers.
- Optimal technological modes for the metallurgical charges briquetting are formulated.

GRAPHICAL ABSTRACT

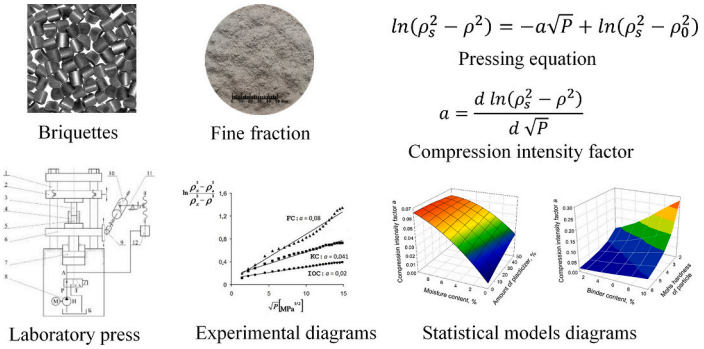

ARTICLE INFO

Keywords:
Non-fired agglomeration
Briquetting
Fine-grained raw materials
Compressibility
Multiple non-linear regression
Design of experiment
Optimization

ABSTRACT

This paper represents the study of the briquetting process optimization of metallurgical charges. A new measure of briquettes' quality – the compression intensity factor, is developed. Using the design of experiments, the nonlinear relationships are established of given factors: the content of plasticizer and moisture, hardness of the particles, dynamic viscosity of the liquid binder, amount of carbonaceous component and the average particle size in the charge. The adequateness of the models was estimated. It is shown that the greatest influence on compressibility has the hardness of the particles while the dynamic viscosity of the liquid binder has a minimum effect. An effective way to control the briquetting process is to change the content of the plasticizer and moisture. In the case of iron-carbon mixtures, it is necessary to control simultaneously the content of carbonaceous material and the particle size of both components. The article provides detailed recommendations on results implementation.

1. Introduction

Currently, the world community is undertaking serious efforts to prevent an environmental catastrophe on a planetary scale [1,2]. The Paris Agreement defined a global strategy to curb the increase in the average temperature on the Earth, providing for the reduction of greenhouse gas emissions to a level that can be naturally recycled by the biosphere [3]. According to the Swedish Environmental Protection

* Corresponding author.
E-mail address: pavlo.krot@pwr.edu.pl (P. Krot).

https://doi.org/10.1016/j.powtec.2022.118025
Received 26 May 2022; Received in revised form 9 October 2022; Accepted 12 October 2022
Available online 18 October 2022

Agency, the share of ferrous metallurgy in global greenhouse gas emissions is about 11% [4], most of which is represented by carbon dioxide CO_2 released in an amount of up to 2 tons per 1 ton of steel produced [5]. >80% of these CO_2 emissions are generated during steel production according to the scheme "production of coke and agglomerated iron-bearing materials – blast furnace – basic oxygen furnace", where fossil fuels are used as raw materials, heat sources and reducing agents in the production of coke, high-temperature agglomeration of iron-bearing materials and blast furnace ironmaking [4]. Thus, reducing the use of fossil fuels in the iron and steel industry is one of the most important directions on the way to the decarbonization of the industry as a whole.

The formulated problem can be solved by developing the following most-promising innovative technologies:

- non-firing agglomeration of iron ore raw materials and coke breeze;
- modernization of the blast-furnace process with recycling of converted top gas (Top gas recycling BF [6,7]);
- high-intensity liquid-phase reduction of iron (HIsmelt, HIsarna [8,9]);
- production of sponge iron through direct solid-phase reduction of oxides with converted natural gas (Midrex, HYL [10,11]) or hydrogen (HYBRIT, H2FUTURE [12]);
- hydrometallurgical extraction of iron from ultrafine ores by leaching and electrolysis (SIDERWIN, ULCOWIN [13,14]).

The processes of high-intensity liquid-phase reduction of iron, as well as hydrometallurgical technologies and direct solid-phase reduction followed by smelting in electric arc furnaces, can reduce the intensity of CO_2 emissions into the atmosphere up to 60–95%, at the same time, the modernization of the existing technology for the production of crude iron can only reduce emissions by 25–60% [4]. Therefore, proposals to exclude a blast furnace from the metallurgical cycle, to meet global climate goals, seem to be strategically justified [15].

However, the possibility of immediate replacement of the blast furnaces is doubtful, since alternative iron reduction technologies, some of which had been developed >50 years ago, have not yet reached an industrially significant production scale. As the authors rightly point out [16], the replacement of a blast furnace with COREX, DIOS and HIsmelt technologies, which impose less stringent requirements on raw materials and fuel, and do not require significant financial costs to maintain smelting units in working condition, was expected back in the 1990s. However, this has not happened so far due to the constant improving the blast furnace process and its productivity increasing. Currently, the main part of steel in the world – about 70% – is smelted in a basic oxygen furnace from blast furnace crude iron [17].

The nearest realistic prospect for the decarbonization of ferrous metallurgy is the modernization of the blast-furnace process, as well as the development of non-firing methods for the production of agglomerated iron ore and metallurgical fuel. It should be noted that in the total amount of average annual CO_2 emissions generated during the production of steel according to the scheme "production of coke and agglomerated raw materials - blast furnace - basic oxygen furnace", 48% are emitted by a blast furnace, and 33% are formed during high-temperature agglomeration of iron ore raw materials and production of coke [14]. Thus, the replacement of high-temperature methods of agglomeration (sintering, roasting of pellets) and the cutting down of coke production due to the development of technologies for non-firing agglomeration of iron ore raw materials and coke breeze is an urgent task for modern metallurgy.

The fundamental difference between non-firing agglomeration and high-temperature methods lies in the hardening of aggregates of small particles using binders based on types of cement and molecular-dispersed systems. The latest is usually divided into binders of organic and inorganic origin. Such methods are often called "cold" since they do not require the formation of a high-temperature binder, i.e. a mineral melt.

The known methods of non-firing agglomeration: briquetting in roller presses [18–23], production of cold-bonded pellets [24], vibration pressing [25,26] and stiff vacuum extrusion [27,28] have received the greatest industrial application in metallurgy. The most universal, in terms of requirements for raw materials, is the method of briquetting in roller presses. This method allows agglomerating not only iron ore materials with high specific gravity and lyophilic particle surface but also the entire range of other charge components, which are used in ferrous metallurgy. For example, carbon-containing materials (coke, stone and brown coals, peat, etc.), fluxes (limestone, active lime, fluorite, etc.), refractory clays, as well as fine-grained wastes of the main technological stages, both individually and in mixtures with a wide range of proportions. Inorganic binders (liquid glass, polymer compositions, etc.) and organic substances (molasses, resins, starch, etc.), types of cement are used as binders for roller briquetting, and briquetting without the use of binders is also possible in some cases.

Among the advantages of roller briquetting in comparison with other methods of non-firing agglomeration, it is necessary to mention the following [29]:

- the increased density and strength of briquettes due to the influence of loads that lead to destruction and subsequent uniform redistribution of particles in the volume of the briquette, a decrease in porosity and an increase in the total contact surface of the particles;
- the reduced moisture content and lower consumption of binders, due to the achievement of a denser packing of particles, as well as the elimination of the strict necessity to use only types of cement (that is typical for other types of non-firing agglomeration);
- the uniformity of the size and shape of the roll briquettes improves the gas flow characteristics of the charge column in the blast furnace stack;
- the roller press briquettes are less prone to abrasion wear, in comparison with briquettes, formed by vibration or extrusion due to the near-spherical shape (see Fig. 1);

One of the most important quality characteristics of agglomerated raw materials for the blast-furnace process is cold strength (i.e. ability to withstand compressive load and resistance against tumbling), which

Fig. 1. Metallurgical briquettes are produced in a roller press.

directly depends on its density [17,30,31]. Therefore, the investigation of the dependencies of the metallurgical raw materials compression process serves as the solid basis for optimizing the technology of fine-grained materials briquetting.

The issue of the compressibility of composite metallurgical charges with different binders has been relatively little studied to date. A significantly larger amount of studies is devoted to the problems of agglomeration of pharmaceutical, ceramic metal powders or agricultural materials via either compacting or pelletizing. The problem of assessing the compression characteristics of various fine and granular materials has been examined through the application of known compression models by authors [32] and via the development of a new compression equation in paper [33]. The effect of the influence of different binders on the mechanical characteristics of roll-compacted dry granules has been explored and the most effective binders were detected in the work [34]. The authors in [35] examined the effects of both the composition and size of granules on compactability of binary powder mixtures. Several studies devoted to the development of optimization strategies for the production process: in paper [36] considered the effect of fluxes addition on physical and metallurgical properties of iron ore pellets, while in work [37] an influence of organic binders on roll compaction process of magnesia powder has been elaborated. Factorial experimental design has been successfully used in [38] to understand fully the effect of process variables on DDGS granulation behaviour and quality characteristics of granules. Applying the Box-Behnken experimental design plan and Response Surface Methodology, authors [39] solved the dual goal of modelling with subsequent optimization of technological process parameters during green pelletisation of fine iron ore.

In the field of research on the compression of fine-grained metallurgical materials, the most known studies are usually devoted to solving specific technological problems. Authors of the study [40] concluded, that for producing briquettes from active lime screenings at an industrial scale, a coarse fraction of material should be preferred and the gap between rolls should be increased, which allows for minimizing the pseudo fluidization effect of air counter flow on small particles, while improving roll briquetting productivity simultaneously. The research conducted by authors [41] made it possible to transform dispersed ferroalloy dust into charge material for an electric furnace. By the results of the study, it was revealed that the use of refractory cement instead of Portland cement, allows for obtaining briquettes with decent degradation resistance at high temperatures. In addition, a standard test, which consists of a combination of CSR and TUMBLER tests, has been developed to estimate briquettes' durability in the furnace. A way of tackling dust formation during heat treatment of kaolin clay in rotary refractory furnaces was developed in the study [42]. Authors [42] proved the effectiveness of briquetting this material at the determined moisture content in the roller press with the claw-grooved configuration of formation elements. As a result, the quality characteristics of briquettes (yield from rolls, green strength, density) increased, while breakage and dust formation during heat treatment significantly lowered. In paper [43], it was determined the range of Fe/C ratio that allowed obtaining commercially fit briquettes, composed of a mix of low-grade iron ore with coke breeze in certain proportions. Production of such briquettes is useful for not only resource preservation but also helps to increase the productivity of iron and steel making, due to the fast oxide reduction rate of briquettes. Authors in [44] conducted research to improve the efficiency of metallurgical coal fines usage by producing carbon composite iron ore briquettes. The values of coal content, particle sizes, heating rate and briquetting pressure, necessary to obtain optimal results have been determined. In the research study [45] a technological mode for briquetting a mix of BF dust, furnace slag and gas-cleaning dust has been developed. The authors determined the optimal type of binder (which happens to be a refinery waste product) and its amount enabling the manufacturing of commercially fit briquettes.

The findings of the abovementioned papers are of significant practical interest, but still, there is no a systematic approach to researching the complex multifactorial process of metallurgical charges compressing that hinders further development and optimization of briquetting technologies based on mathematical models of materials compressibility.

The purpose of the present paper is to represent planned experimental research, the developed statistical models and analysis of the dependences of the metallurgical charges compressibility on the most significant technological factors. The obtained results allow subsequent determination of ways to increase the compressibility of charge mixtures, the creation of technological modes, improvement of mechanical characteristics of briquettes and construction of pressing equipment.

2. Materials and methods

The fine-grained materials of the four different technological groups were used for the research: iron-containing (iron ore concentrate and furnace scale), fuel-reduction (medium-volatile bituminous coal and coke breeze), fluxing (fluorite concentrate grade FF-95) and plasticizer (kaolin clay). Raw materials of the research are shown in Fig. 2 and Fig. 3. In the course of pre-experimental preparation, fine-grained materials were dried to complete loss of moisture. The granulometric composition of raw materials was determined by sieve analysis in laboratory conditions at the Iron and Steel Institute of NASU. The granulometric composition of iron ore and fluorite concentrates was determined in the laboratories of the raw material suppliers.

The granulometric composition of fine-grained materials is as follows.

Furnace scale: 11.4% (0–0.25 mm); 10% (0.25–0.5 mm); 15.4% (0.5–1 mm) 28.5% (1–2 mm); 20.3% (2–3 mm); 14.4% (3–5 mm).

Coke breeze: 7.6% (0–0.25 mm); 6.5% (0.25–0.5 mm); 8.2% (0.5–1 mm); 21% (1–2 mm); 29.5% (2–3 mm); 27.2% (3–5 mm).

Kaolin clay and coal: 100% (0–0.25 mm).

Iron ore concentrate: 94.7% (0.044–0.074 mm).

Fluorite concentrate: 36% (0–0.028 mm); 32% (0.028–0.063 mm); 21% (0.063–0.1 mm).

The information on the chemical composition of materials was obtained from raw material suppliers and presented in Table 1.

The mixing of charges was carried out in a laboratory mixer until the state of maximum homogenization was reached. Briquettes weighing 10–50 g were formed without heating in a closed steel mould by one-sided pressing. Pressing was carried out without holding pressure, at a constant strain rate of 22.5 mm/min, until a force of 75 kN was reached. Such force in the given experiment corresponds to a pressure of 220 MPa. The inner diameter of the cylindrical die is 20.9 mm, the channel depth is 57.05 mm, and the ends of the punches are flat. The laboratory press unit is assembled based on a universal testing machine TsD − 10 with a nominal force of 100 kN and the ability to change the speed from 0.05 mm/s to 6 mm/s (Fig. 4).

The experimental data were recorded in the form of compression graphs in the "pressure-shrinkage" coordinates (Fig. 5). At the endpoint of the graph, the dimensions of the briquette are characterized by the final shrinkage $h_{shr.f}$ and the height of the briquette h_{br}, the sum of which is equal to the initial height of the material filling h_0. The density of the briquette was calculated from its parameters at the end of the compression process. Based on the final density, intermediate values of briquette density were calculated corresponding to the current shrinkage $h_{shr.i}$. Each point of the experiment is an average of the data from five experiments. Thus, to analyse the experimental results, the experimental pressing curves were presented in the form of dependencies $P = f(\rho)$.

A detailed description of the laboratory setup and procedures for conducting experiments and processing experimental data are given in the work of the authors [46].

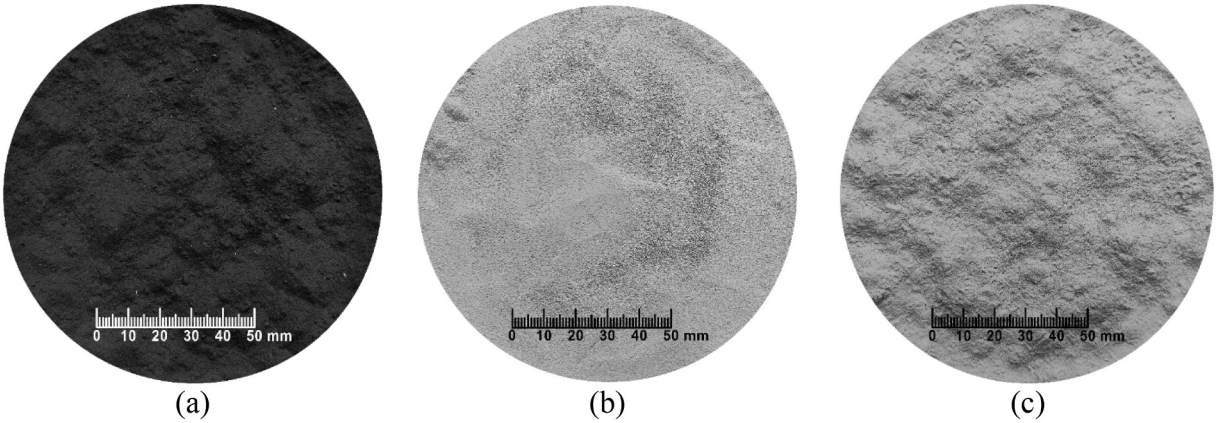

Fig. 2. Fine fraction materials used in the research: a) iron ore concentrate; b) kaolin clay; c) fluorite concentrate.

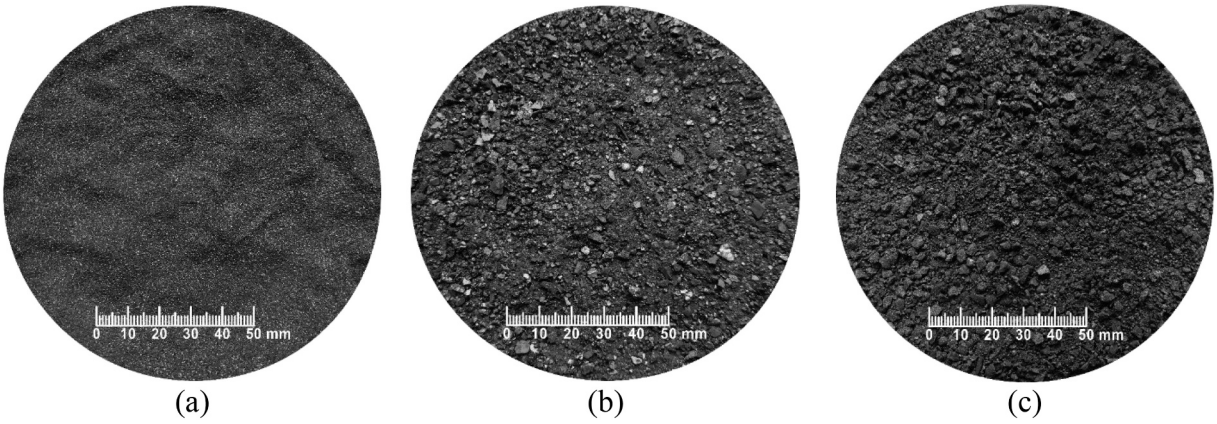

Fig. 3. Fine fraction materials used in the research: a) coal; b) furnace scale; c) coke breeze.

Table 1
Chemical composition of raw materials*

Raw material	Content weight, %								
	FeO	Fe_2O_3	SiO_2	Al_2O_3	CaO	MgO	CaF_2	Fe_{total}	C_{total}
Iron ore concentrate	19.4	71.1	8.4	0.69	0.25	0.1	–	64.8	–
Kaolin clay	–	44.02	50.56	0.22	0.41	0.95	–	–	–
Fluorite concentrate	–	0.11	2.7	0.18	–	–	96.15	–	–
Coal (ash)	–	12.97	53.32	15.88	5.53	1.26	–	–	86.88*
Furnace scale	40	–	2	–	0.47	–	–	60	0.76
Coke breeze (ash)	–	25.8	42.8	20.56	4.67	1.8	–	–	94*

* The carbon content in coal and coke breeze is given for dry ash-free mass of materials.

3. The concept of research, planning of experiments

Based on the available practical experience in the field of briquetting and analysis of literary sources [5,19,21,30,31,45–51], the factors that have the most significant impact on the process of compression of metallurgical charges are determined:

1) the content of the plasticizer and the moisture content of the charge mixture;
2) the fractional content in the mixture and fineness of ferrous and carbonaceous materials;
3) the physical properties of raw materials with binders and binder content.

Taking into account the diversity of the list of fine-grained materials for briquettes in the metallurgical industry, the decision was made in the work on the expediency of modelling the action of the selected factors by using a limited number of model materials. The concept of using selected materials as representatives of groups united based on their common technological purpose or certain physical properties is based on the statistical idea of a sample population, as some part of the general population, which has the property of representativeness.

3.1. The first group of factors

The influence of plasticization of the charge mixture on the course of the compression process is investigated. The degree of plasticization is determined by the content of the plasticizer and the moisture content of the mixture. Kaolin clay was chosen as the model charge plasticizer, which changes into a viscous-plastic state upon contact with water. From a rheological point of view, this material reflects the properties of moistened mineral binders (cement slurries, bentonite clay, clay-cement

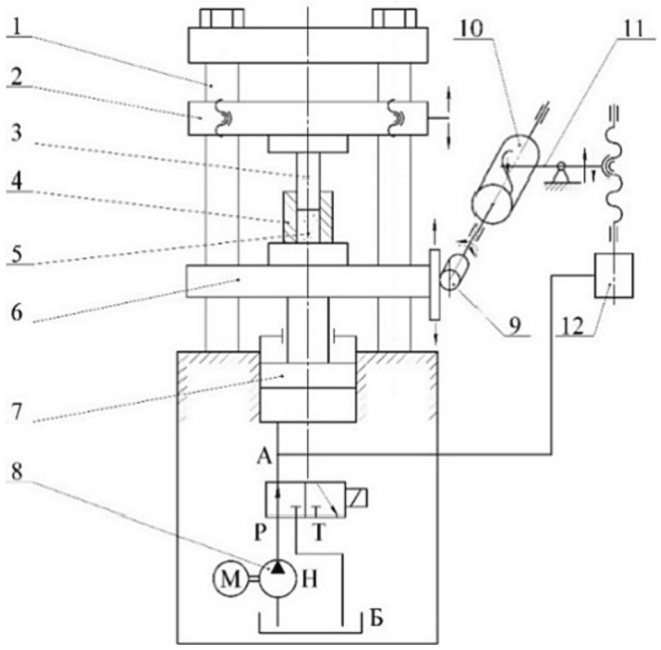

Fig. 4. Scheme of the laboratory press unit: 1 – column; 2 – traverse movable; 3 – punch; 4 – matrix; 5 – charge; 6 – hydraulic cylinder traverse; 7 – hydraulic cylinder; 8 – pump; 9 – transmission mechanism; 10 – recorder drum; 11 – recorder pen; 12 – pressure transducer.

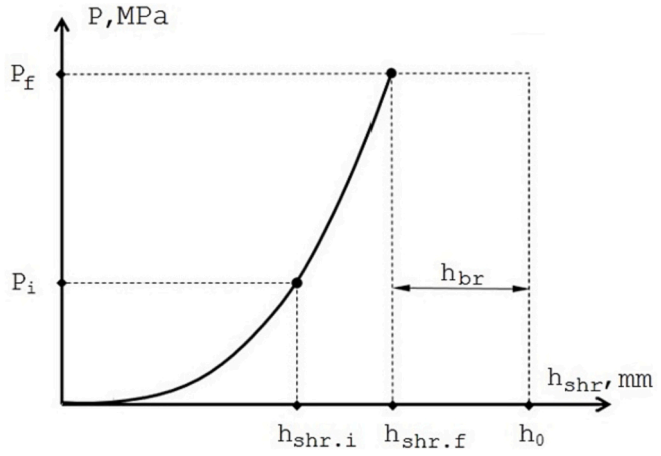

Fig. 5. Qualitative graph of fine-fraction material compression.

compositions) and poor iron-containing industrial waste (sludge, aspiration dust, etc.). The main component of a metallurgical briquette is, as a rule, ferrous raw material. Magnetite concentrate, which is typical in terms of iron content and size of ore particles, was chosen as the model of such material.

3.2. The second group of factors

The influence of the content and particle size of components on the process of compression of the iron-carbon charge is investigated. Furnace scale and coke breeze were chosen as models of ferrous and carbonaceous raw materials, since, due to the high content of useful components, they are most often used in briquetting as sources of iron and carbon.

3.3. The third group of factors

The effect of the nature of the mixture components on the resistance of the charge to external deforming effects during compression is studied. To describe the physical properties of raw materials, Mohs hardness *HM* was used, since this indicator characterizes the resistance of particles to fragmentation and, therefore, reflects the strength of the interatomic bonds of the substance of the solid phase. The following materials were chosen as model materials: coal, fluorite and magnetite concentrate. Each of the selected materials represents a group of raw materials with a separate technological purpose in metallurgical stages: fuel-reduction, fluxing and iron-containing groups. At the same time, coal is characterized by the lowest hardness $HM = 2$, magnetite concentrate - the highest $HM = 6$, and fluorite concentrate occupy an intermediate position $HM = 4$.

To describe the physical properties of liquid binders, dynamic viscosity η is used, since this indicator serves as a measure of the shear resistance of liquid layers. The preliminary research carried out by the authors showed that sugar beet molasses is characterized by the highest viscosity $\eta = 657$ mPa·s. At the same time, it is known that the least viscous liquid binder is water $\eta = 1$ MPa s. The intermediate value of viscosity is equal to $\eta = 329$ MPa s. Such a viscosity at a temperature of about 20 °C has a 69% aqueous solution of sugar.

Experimentally, the compressibility of metallurgical charges with a change in these factors was determined using elements of the theory of experiment planning [52,53]. For the formulated tasks, three planning matrices were used for non-compositional plans of the second order: a two-factor simplex-summable C-C2 and a three-factor Box-Benkin B-B3 plan. The natural values of the factors for the respective levels are shown in Table 2.

4. Development of compression intensity factor

It is known that in the theory of elasticity, the measure of the quantitative description of the compressibility of a solid-state matter is the coefficient of all-round compression: $\beta = \frac{1}{\rho}\frac{d\rho}{dP}$ [54]. In the theory of compression of powder materials, it is also accepted to identify the concept of compressibility with the intensity of compression, that is, with the rate of change in the density of a powder with increasing compression pressure [55]. However, if the compressibility of solids is a constant value in a significant pressure range [56], then in the case of compression of powder materials, the intensity of compression is constantly changing due to the staged nature of the process of their deformation. It takes maximum values at the initial and minimum values at the last stages of the process [57,58]. Therefore, it is advisable to use

Table 2
Factors and levels of their variation in the plan matrices of experiments.

No.	Plan	Names of factors	Factor levels			Variation intervals
			−1	0	+1	
1.	C-C_2	Amount of plasticizer, X_1 [%]	0	25	50	25
		Moisture content, X_2 [%]	0	5	10	5
		Amount of carbonaceous material,* X_3 [%]	10	50	90	40
2.	B-B_3	Average particle size of ferrous material, X_4 [mm]	1	2.5	4	1.5
		Average particle size of carbonaceous material, X_5 [mm]	1	2.5	4	1.5
		Mohs hardness of particle *HM*, X_6	2	4	6	2
3.	B-B_3	Binder content, X_7 [%]	1	5.5	10	4.5
		Dynamic viscosity of binder η, X_8 [mPa·s]	1	329	657	328

* In the plan of experiment No. 2, the mixtures are bicomponent, so the sum of the fraction contents of ferrous and carbonaceous material is 100%.

the dimensionless coefficients of the pressing equations, which make it possible for a linear approximation of the experimental compression curves of most fine-grained materials in a wide range of pressing pressures.

In the paper of the authors [59], a pressing equation was proposed, which, with an average accuracy of $R^2_{av} = 0.977$, describes experimental diagrams of compression for charges, composed of raw materials used in ferrous metallurgy (iron-containing, fuel-reducing and fluxing):

$$ln\left(\rho_s^2 - \rho^2\right) = -a\sqrt{P} + ln\left(\rho_s^2 - \rho_0^2\right), \quad (1)$$

where ρ – density of briquette, g/cm^3; ρ_0 – loose bulk density of charge, g/cm^3; ρ_S – true density of particles, g/cm^3; P – compression pressure, MPa; a – compression intensity factor. The coefficient a characterizes the tendency of fine-grained material to reduce its volume when pressing pressure is applied and is defined as $a = \frac{d\, ln\left(\rho_s^2 - \rho^2\right)}{d\sqrt{P}}$. In the case of compressing a mixture of fine-grained materials, the variable of ρ_S is determined as the weighted arithmetic mean value of true densities of particles of mixture components. Thus a ρ_S of the mixture is defined as follows: $\rho_S = \frac{\sum_i^n \rho_{Si} * x_i}{\sum_i^n x_i}$, where ρ_{Si} – the true density of particles of certain material in the mixture; x_i – the content of certain material in the mixture.

To determine the compression intensity factor a, it is necessary to linearize the experimental pressing curve of powder material (see Fig. 5), specifically it should be transformed using Eq. (1). Consequently, experimental data should be presented in coordinates: $ln\left(\rho_s^2 - \rho^2\right) = f\left(\sqrt{P}\right)$ and $ln\frac{\left(\rho_s^2 - \rho_0^2\right)}{\rho_s^2 - \rho^2} = f\left(\sqrt{P}\right)$. Then it is needed to perform a linear approximation and calculate the tangent of the slope of the approximating straight line, the numerical value of which is equal to the compression intensity factor a. The smaller the angle of inclination of the approximating straight line to the abscissa axis, along which the pressure function is plotted, the smaller the coefficient a and the less intensively the density of the powder material increases during pressing. Theoretically, if the straight line is horizontal, then the powder material does not compress at all when pressure is applied and can be characterized as unrestrictedly rigid. Otherwise, if the straight line is vertical, then the material is infinitely soft. However, absolutely soft or hard materials do not exist in nature, so all real fine-grained materials have an intermediate characteristic.

The compression diagrams of the fine-grained raw materials in an air-dry state are shown in Fig. 6 and Fig. 7. The greatest rigidity is characterized by iron ore concentrate $a = 0.02$, and the smallest by furnace scale $a = 0.097$ and coal $a = 0.092$.

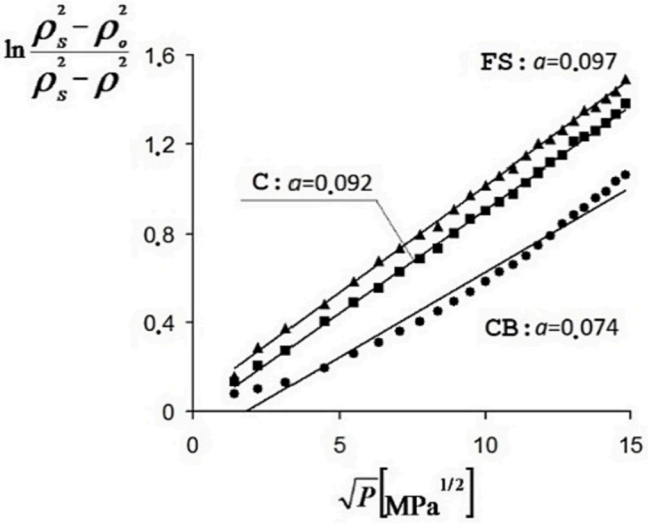

Fig. 7. Compression diagrams for furnace scale FS, coal C, coke breeze CB.

Experimental confirmation of the possibility of using the coefficient a as an indicator of the compressibility of powder materials is the high level of correlation established when compared with the compressibility index according to the ISO 3927:2017 standard [60] – the density of materials achieved at the same pressure. The data in Fig. 8 indicate the presence of a functional relationship between the compression intensity factor a and the relative density $D = \rho/\rho_S$ achieved by the mixture at a pressing pressure $P = 100$ MPa. To carry out the correlation analysis, we used experimental data in form of compression diagrams for 79 charge mixtures, composed of various fine-grained materials of the mining and metallurgical complex [61].

Compared to the compression index according to ISO 3927:2017, the compression intensity factor a has the following advantages:

- firstly, coefficient a has a clear physical meaning, it is theoretically more justified and also it is suitable for comparing different charges, since coefficient a an integral characteristic of the entire compression process, not only some of its separate stages;

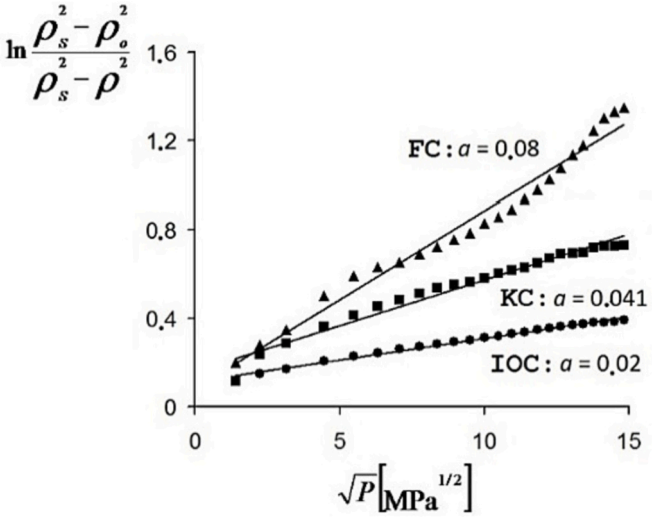

Fig. 6. Compression diagrams for fluorite concentrate FC, kaolin clay KC and iron ore concentrate IOC.

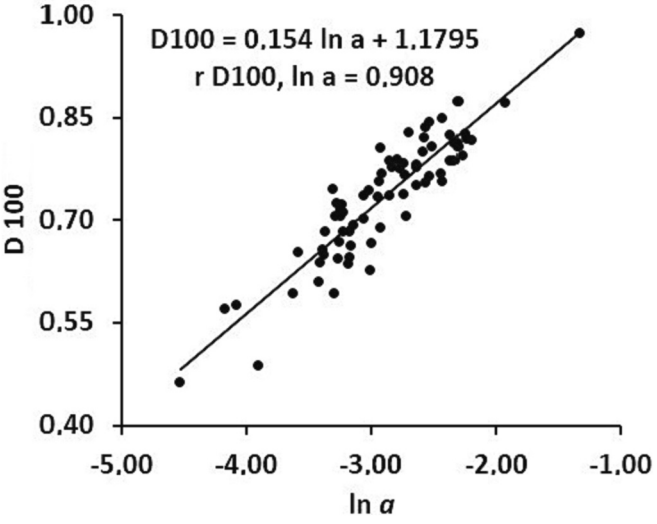

Fig. 8. Relationship between compression intensity factor a and relative density of compressed powders D at a pressure of 100 MPa.

- secondly, the coefficient a is more universal from a practical point of view since it can be used for already examined charges and powder materials, the experimental data on compression which were obtained in various pressure ranges and published in the form of tables, as well as graphic diagrams "pressure - density" in scientific and technical publications.

The proposed coefficient a can serve as the basis for the quantitative classification of charges with different physicochemical and physical and mechanical properties according to a single compressibility characteristic. By the analysis of the coefficient a change, it is possible to evaluate the effectiveness of both the preparation of charges for pressing and various compression methods.

5. Results and discussion

The experiments were implemented following the plan matrices C—C2 and B—B3 for the selected factors (see Table 2). The results of the experiments are given in Table 3, Table 4 and Table 5.

After the implementation of the experimental plans, a statistical analysis of the obtained data was performed and regression coefficients were determined for second-order polynomials that describe the configuration of the response function surface for the selected factors in given ranges of their values.

The general form of a second-order polynomial statistical model is as follows:

$y = b_0 + \sum_1^k b_i x_i + \sum_1^k b_{ii} x_i^2 + \sum_{i<j}^k b_{ij} x_i x_j$, where b_0, b_i, b_{ii}, b_{ij} – regression coefficients; x_i, x_i^2 – factors and their squares; $x_i\, x_j$ – the effect of the interaction of factors.

Mathematical models have been obtained that describe the dependence of the compressibility of metallurgical charges on:

- the amount of plasticizer content and moisture content:

$$a = 0.0492 + 0.0045X_1 + 0.0234X_2 - 0.0062X_1X_2 - 0.0012X_1^2 - 0.0078X_2^2 \quad (2)$$

- the amount and particle size of ferrous and carbonaceous materials:

$$a = 0.0565 - 0.0086X_3 + 0.0049X_4 + 0.0073X_5 - 0.0145X_3X_4 + 0.0037X_3X_5 - 0.0077X_4X_5 + 0.0393X_3^2 - 0.0006X_4^2 + 0.0038X_5^2 \quad (3)$$

To apply the obtained models, it is necessary to present the factors in a coded form. The transition to coded values from natural ones can be easily performed, using the values of the variation intervals and the zero levels of factors in their natural form from Table 2 through the known formula [53]:

$$X_i^{coded} = \frac{X_i^{natural} - X_i^{zero}}{I_i} \quad (4)$$

where X_i^{coded}, $X_i^{natural}$ – values of the i-th factor in coded and natural forms on a given level, respectively; X_i^{zero} – values of i-th factor in natural form on zero level; I_i – variation interval of i-th factor in natural form.

Analysis of the experimental data on the dependence of charge compression on the properties of fine-grained materials, the amount and properties of the liquid binder (Table 5) showed that, in comparison with other factors, the change in the dynamic viscosity of the binder has little effect on the charge compression intensity factor a. So, with the constancy of other factors, the change in viscosity from the minimum $\eta = 1$ mPa·s to the maximum value $\eta = 657$ mPa·s led to a change in the coefficient a in the range of 4.4–26.3% (experiments No. 6 and 5, No. 10 and 9, respectively). At the same time, the change in the amount of the liquid binder in the range from the smallest to the largest level is accompanied by a change in compression intensity factor from 196.8% to 319.3% (experiments No. 2 and 1, No. 4 and 3, respectively). The change of material hardness in the range from lower $HM = 2$ to upper $HM = 6$ level contributes to a change in compression intensity factor by 749.9%, i.e. by 7.5 times (experiments No. 3 and 1). Thus, it was found that factor X_8, which represents the properties of a liquid binder, does not significantly affect the compressibility of metallurgical charges, which made it possible to exclude it from further consideration in the present research.

After the exclusion of factor X_8, the array of experimental data from Table 5 was subjected to regression analysis using the Sigma Plot 12.5 software package. The resulting nonlinear mathematical model has the form of a Lorentz function and describes the dependence of charge compression on the hardness of particles of fine-grained materials and binder content:

$$a = \frac{5.8431}{\left[1 + \left(\frac{X_6 + 0.6902}{0.6245}\right)^2\right]\left[1 + \left(\frac{X_7 - 11.5630}{6.9808}\right)^2\right]} \quad (5)$$

It should be noted that to apply model (5), the factors X_6 and X_7 must be presented in their natural form.

Table 3
Influence of the amount of plasticizer and moisture content on the charge compressibility.

Factors and response function	Experiment number						
	1	2	3	4	5	6	7
X_1, %	0	50	37.5	37.5	12.5	12.5	25
X_2, %	5	5	9.35	0.65	9.35	0.65	5
Compaction intensity factor a	0.040	0.056	0.059	0.024	0.067	0.021	0.05

6. Verification of statistical models

The reproducibility of the processes in the implementation of experimental plans for the obtained models was checked by evaluating the uniformity of dispersions according to the Cochran criterion G. The calculated value of the G criterion for model (2) is $G_{calc} = 0.32$, for model (3) $G_{calc} = 0.2468$, and for model (5) $G_{calc} = 0.1311$. Since in all cases the values of the Cochran criterion are less than the tabular $G^{0.05}_{\text{tab}} = 0.9669$, then the reproducibility of the models is sufficient with a 95% probability. The adequacy of the models to the experimental data was checked according to the Fisher F criterion. It has been determined, that for obtained models (2), (3) and (5), calculated values of the F criterion are lesser than the tabular ones. For model (2) $F_{calc} = 3.82 < F_{tab}^{0.05} = 6.59$, for model (3) $F_{calc} = 3.4 < F_{tab}^{0.05} = 3.9$, and for model (5) $F_{calc} = 1.13 < F_{tab}^{0.05} = 3.9$. Thus, the obtained models are adequate at the significance level $\alpha = 0.05$.

The calculated values of the average relative errors for mathematical models (2), (3), and (5) are within the acceptable range of accuracy ($\overline{A} < 8\ldots10\%$) and equals 9.5%, 7.9% and 9.8%, respectively. Values of squared correlation coefficients for models (2), (3) and (5) also are within the acceptable range ($R^2 > 0.9$) and equals 0.961, 0.928 and

Table 4
Influence of the amount and particle size of ferrous and carbonaceous materials on the charge compressibility.

Factors and response function	Experiment number												
	1	2	3	4	5	6	7	8	9	10	11	12	13
X_3, %	90	90	10	10	90	90	10	10	50	50	50	50	50
X_4, mm	4	1	4	1	2.5	2.5	2.5	2.5	4	4	1	1	2.5
X_5, mm	2.5	2.5	2.5	2.5	4	1	4	1	4	1	4	1	2.5
Compaction intensity factor a	0.084	0.087	0.103	0.077	0.101	0.083	0.109	0.105	0.058	0.055	0.08	0.04	0.057

Table 5
Influence of material properties, content and properties of the binder on the charge compressibility.

Factors and response function	Experiment number												
	1	2	3	4	5	6	7	8	9	10	11	12	13
X_6	6	6	2	2	6	6	2	2	4	4	4	4	4
X_7, %	10	1	10	1	5.5	5.5	5.5	5.5	10	10	1	1	5.5
X_8, mPa·s	329	329	329	329	657	1	657	1	657	1	657	1	329
Compaction intensity factor a	0.039	0.02	0.289	0.091	0.037	0.035	0.177	0.156	0.103	0.082	0.031	0.028	0.073

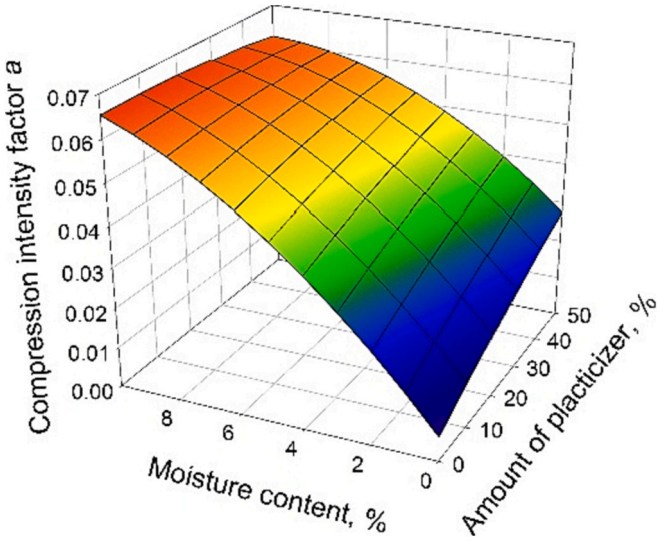

Fig. 9. Charge compression dependence on moisture content and amount of plasticizer.

0.987, respectively. Therefore, the resulting models give a good fit to the experimental data and are accurate enough for practical use.

7. Analysis of statistical models of charge mixtures compressibility

7.1. Model by Eq. (2)

A graphical representation of the dependence of compressibility on the amount of plasticizer and the moisture content of the charge mixture is shown in Fig. 9. The curvilinear nature of the surface of the response function is obvious and it changes unevenly with varying experimental factors. Dependence analysis shows that the minimum compressibility of the charge $a = 0.006$ corresponds to zero moisture content and the absence of a plasticizer. As the values of these factors increase, an increase in compressibility is observed, which is due to two reasons. Firstly, in the presence of a liquid phase, the clay component of the charge is plasticized due to the absorption of part of the water by the crystal lattice of minerals. In their turn this leads to dispersion of the solid phase, the elementary particles of which are separated by interlayers of adsorbed moisture, thus, due to the weakening of the bond between the packages of atoms in the lattice, the work required to deform the macroparticles decreases. Secondly, the water in the pores, capillaries and on the surface of the macroparticles facilitates their mutual sliding during the pressing of the mixture.

As moisture content increases, the effect of the plasticizer addition on compression decreases sharply. Changing the amount of plasticizer from the smallest to the largest leads to an increase in the compressibility of the dry mixture by 4.6 times (from $a = 0.006$ to $a = 0.027$) and practically does not affect the compression of the mixture with 10% moisture (coefficient a equals 0.065 and 0.062, respectively). The maximum compression $a = 0.065$ is achieved at the highest moisture content. It practically does not depend on the amount of plasticizer and is 10 times higher than the minimum compression characteristic of dry charge.

7.2. Model by Eq. (3)

Graphical representation of the dependence of charge compression on the amount and particle size of ferrous and carbonaceous materials are shown in Fig. 10 in the form of two-dimensional sections of the surface of the response function of the three-factor model (3). Each of the images characterizes the compressibility of the charge mixture concerning a pair of factors plotted along the abscissa and ordinate axes, with the third factor fixed at zero level. The analysis of two-dimensional sections gives an idea only about the local extrema of the response function, in areas limited by the set value of one of the three factors of the experiment. For reliable analysis of compressibility for all possible combinations of factors in the given intervals of their variation (see Table 5), it is necessary to determine the global extrema of the response function.

7.2.1. Determination of global extrema of the response function by the model (3)

To determine the global extrema of the function on the set of values that make up the three-dimensional factor space of the model (3), optimization problems were formulated and solved to find the minimum and maximum compressibility of the charge mixture with the limitation of factors: $-1 \le X_i \le 1$. The analytical statement of the problem is as follows:

$$\begin{cases} a = 0.0565 - 0.0086X_3 + 0.0049X_4 + 0.0073X_5 - 0.0145X_3X_4 + 0.0037X_3X_5 - \\ \quad -0.0077X_4X_5 + 0.0393X_3^2 - 0.0006X_4^2 + 0.0038X_5^2 \rightarrow min(max); \\ X_3^2 + X_4^2 + X_5^2 = R^2. \end{cases} \quad (6)$$

where R – the radius of the sphere, defining the boundaries of the

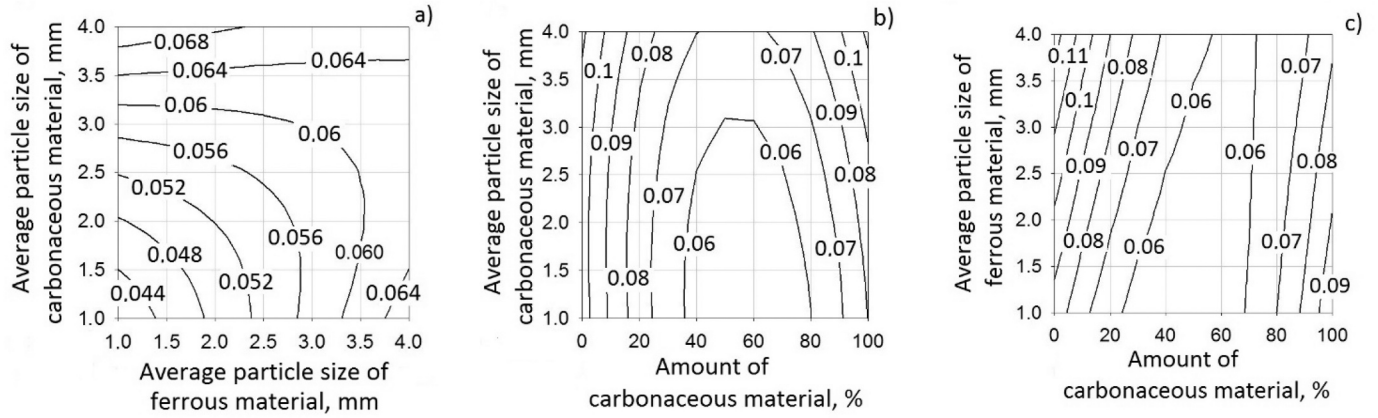

Fig. 10. Compressibility of the charge under conditions: a) equal amounts of ferrous and carbonaceous materials in the mixture; b) average particle size of ferrous material is 2.5 mm; c) average particle size of carbonaceous material is 2.5 mm.

experiment area.

The solution to the optimization problem was performed using the method of indefinite Lagrange multipliers [52,62], following the computational algorithm in which, the objective function F and a system of Eq. (7) were solved. The latest one contains partial derivatives of the function F concerning the independent variables X_3, X_4, X_5 and the indefinite Lagrange multiplier λ:

$$\begin{cases} \dfrac{\partial F}{\partial x_3} = -0.0086 - 0.0145x_4 + 0.0037x_5 + 0.0786x_3 + 2\lambda x_3 = 0; \\ \dfrac{\partial F}{\partial x_4} = 0.0049 - 0.0145x_3 - 0.0077x_5 - 0.0012x_4 + 2\lambda x_4 = 0; \\ \dfrac{\partial F}{\partial x_5} = 0.0073 + 0.0037x_3 - 0.0077x_4 + 0.0076x_5 + 2\lambda x_5 = 0; \\ \dfrac{\partial F}{\partial \lambda} = x_3^2 + x_4^2 + x_5^2 - R^2 = 0. \end{cases} \quad (7)$$

To solve the system of Eq. (7) and calculate the values of the response function of the model (3), the Mathematica 10 software package was used, performing calculations when the radius of the sphere R changed from 0 to 1.

It has been established that the minimum compressibility of the charge mixture is $a = 0.0398$ and is observed at a ratio of carbonaceous to ferrous material as 49:51 and the same particle size of materials equal to 1 mm. Thus, a mixture of fine fractions of the studied materials, taken in approximately equal proportions, exhibits the greatest resistance to compression, which may be due to several reasons. First, fine fractions are characterized by increased values of particle strength and their total contact surface is relatively large. Secondly, when pressing a mixture of unequal strength materials, the destruction of less strong particles while interacting with stronger ones is likely to take place in the very early stages of the process, presumably simultaneously with the redistribution of rigid particles. Thus, destructed less rigid particles are filling voids between more rigid particles and spatial packing with reduced porosity and increased contact surface is forming. At the same time, rigid particles are forming a certain spatial skeleton. Thereby observed smallest compression intensity factor for the mixture (49:51) of unequal strength materials of particle sizes 1 mm is probably due to the simultaneous action of counterpressure from the side of destroyed low-strength particles that filled the pores, and the resistance of the skeleton formed by stronger particles.

The maximum compressibility of the charge $a = 0.1229$ is achieved with a ratio of carbonaceous to ferrous material 10:90 and the same particle size of materials equal to 4 mm. In this case, the process of the mixture compression is determined by the properties of the prevailing component, which are large particles of iron furnace scale. The highest compressibility of this component is explained, on the one hand, by the fact that large particles serve as centres of stress concentration and, therefore, are primarily subject to destruction during pressing. On the other hand, it is caused by the lower compressive strength of the furnace scale compared to coke (corresponding values are 12–20 MPa versus 36–44 MPa, respectively). The maximum charge compressibility according to model (3) exceeds the minimum by 3.09 times.

7.3. Model by Eq. (5)

A graphical representation of the dependence of compressibility on the hardness of mineral particles and the content of the liquid binder in the charge mixture is shown in Fig. 11. This dependence is characterized by a significant curvature of the surface. It indicates that to increase the compressibility of the charge, an increase in the binder content and a decrease in the hardness of particles of fine-grained material are required. The minimum charge compressibility $a = 0.015$ is observed in the case of pressing the charge, represented by a material with particle hardness $HM = 6$ and 1% of binder content. The maximum compressibility $a = 0.285$ is achieved by pressing the mixture with the lowest particle hardness $HM = 2$ and 10% of binder content. The maximum compressibility exceeds the minimum by 18.6 times.

Since, as it is shown above, the viscosity of the binder has almost no

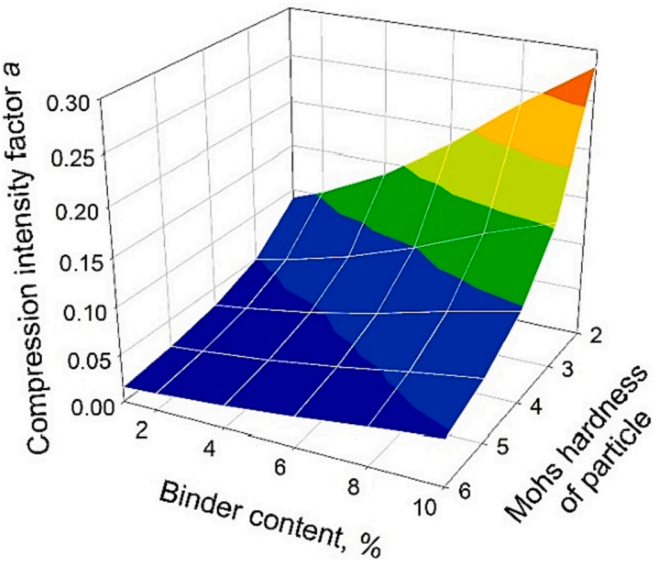

Fig. 11. Charge compression dependence on binder content and hardness of particles.

effect on the compressibility of the charge, it is obvious that the binder content primarily affects the compressibility of the charge. The intensifying effect of this factor is due to a decrease in the internal friction of the charge. At the same time, within the framework of the considered model (5), the physical properties of the fine-grained material particles, namely the strength of bonds in the crystal lattice of minerals, have a decisive influence on the compressibility of the charge. Changes in the binder content are rather enhancing the effect of particles' physical properties on charge compressibility. So, if a change in the particle hardness from $HM = 6$ to $HM = 2$, with a binder content of 1%, leads to an increase in the compression intensity factor by 6 fold (from $a = 0.015$ to $a = 0.091$), then a further increase of the binder content to 10% increases charge compressibility only 3.13 times ($a = 0.285$).

8. Technological recommendations

The performed analysis of mathematical models (2), (3) and (5) shows that the process of compression of metallurgical charges, in addition to the main factor, which is the applied external pressure, is significantly affected by the characteristics of the charge mixture and liquid binder additives, which makes it possible to make some generalized technological recommendations.

When pressing a two-component charge mixture of fine iron ore material (iron ore concentrate or fine ore) and a substance that exhibits plastic properties when moistened (bentonite and other clays, sludge, tailings, and other similar industrial waste), an increase in the moisture content and plasticizer contributes to an increase in the compressibility of the mixture. However, at relatively high values of moisture content (>6–7%), the amount of plasticizer no longer has an intensifying effect on compressibility (Fig. 9).

In the production of two-component iron-carbon briquettes, a significant increase in the compressibility of the mixture can be achieved with a simultaneous increase in the particle size of the materials and the growth of content of one of the components over 80%. The exact ratio of the proportion of carbonaceous to ferrous material in the mixture, which is necessary to achieve the highest compressibility, depends on the size of the materials. For example, as production practice shows, most of the materials for briquetting have an average particle size in the range of 2–3 mm. The highest compressibility of such charges is achieved when using "pure materials", that is, when the mixture contains either 0% or 100% of the carbon component (Fig. 10b and Fig. 10c). At the same time, the maximum value of the compression intensity factor, for the examined range of particle sizes and the content of charge components is achieved, as mentioned above, at the proportion of carbonaceous to ferrous material equal 10:90 and an average particle size of both components equal to 4 mm. The lowest compressibility is observed at the minimum particle size of the materials and approximately equal content of them in the mixture (Fig. 10a).

In the case of briquetting a mono-component charge, the highest compressibility is achieved with a simultaneous decrease in particle hardness and an increase in the content of the liquid phase in the charge, while the type of liquid-phase additive has practically no effect on compressibility (Fig. 11).

9. Classification of compressibility factors

Taking into account the results, obtained in the present research, it seems possible to combine the examined factors into three groups and rank them in order of decreasing influence on the compressibility of charge mixtures (see Table 6).

The above classification of compressibility factors needs further development and refinement. It is necessary to expand the list of physical properties of particles of charge components, since, in addition to the nature of a solid-phase substance; the densification of a mixture is affected by porosity, density, electromagnetic properties of particles and other factors. In addition, the Mohs hardness of particles, chosen in present research as a factor, reflecting the nature of a solid-phase substance, is of little use for characterizing multicomponent metallurgical charges, which include minerals of varying complexity, metals and alloys, organic carbonaceous materials and their pyrolysis products [63,64].

Table 6
Classification of charge compressibility factors.

No.	Generalized names of factors	Factor Examples
1.	Material properties of the charge mixture	
1.1	Component composition of the charge	Amount of plasticizer X_1 and carbonaceous material X_3 in a bicomponent iron ore charge mixture
1.2	Physical properties of particles of charge components	Mohs particle hardness X_6
2.	The liquid phase of the charge	
2.1	Amount of liquid phase	Moisture content X_2 and binder content X_7
3.	Individual and collective properties of particles	
3.1	The particle size of charge components	The particle size of ferrous material X_4 and carbonaceous material X_5 in a bicomponent charge mixture
3.2	Other particle properties	

Therefore, promising directions for further research are as follows. Firstly, the search for some single factor that makes it possible to take into account the variety of types of chemical bonds of the substance of different materials particles. Secondly, a subsequent study of this factor's effect on the compressibility of fine-grained materials and charge mixtures, which are comprised of these materials. In this case, it is necessary to use advanced scientific developments, such as, e.g., the core-electron theory of the structure of minerals by V.V. Zuev [65]. It should be noted that the group of individual and collective properties of charge particles includes, in addition to size, several other factors. The effect of these factors on the compressibility of fine-grained materials also needs to be studied. As shown by our preliminary analysis of the results of works [66–68], the compressibility of charges can be significantly affected by the shape of particles, the characteristics of their surface and the distribution of particles by size (primarily the ratio of mass fractions and linear sizes of particles of adjacent fractions).

10. Conclusions

Currently, about a third of the total CO_2 emissions from the iron and steel industry come from sinter plants and coking plants. A promising direction of decarbonization in the preparation of charge materials is non-firing agglomeration, which does not require the use of fossil fuels as a heat source. The performed research is devoted to the optimization of the technology of cold briquetting of metallurgical materials in roller presses.

A new factor of the compressibility of fine-grained materials has been developed, namely the compression intensity factor a, which characterizes the ability of the charge to reduce volume when exposed to external pressure. The proposed factor is an integral characteristic that takes into account the staging character of the process of compression of powder materials. The coefficient a can be used to classify charges and fine-grained materials based on a single measure of their compressibility, as well as to assess the initial technological state of charge mixtures and the effectiveness of their preparations for briquetting.

Using the methods of physical and mathematical modelling (experiment planning, nonlinear programming and regression analysis), the dependence of the compressibility of metallurgical charges on the following technological factors is studied: the content of plasticizer and the moisture, the hardness of mineral particles, the dynamic viscosity of the liquid binder, the amount and particle size of ferrous and

carbonaceous charge components. Statistical models have been developed with an average relative error of <10% and a squared correlation coefficient greater, than 0.9. Obtained models, with a 95% probability, have sufficient reproducibility by the Cochran criterion and adequacy by the Fisher criterion. The optimal values of technological factors are determined.

It has been established that an increase in the moisture content indefinitely increases the compressibility of the charge, and an increase in the plasticizer amount has a similar effect only when the charge moisture content is <6–7%.

When pressing an iron-carbon-containing bicomponent batch mixture, a decrease in compressibility is observed with a decrease in particle size and with changes in component contents towards equalization of their shares in the mixture. Namely, the lowest compressibility was achieved with a ratio of materials' proportions of approximately 50% to 50% and a minimum material size of 1 mm. While the highest compressibility of the charge was achieved with a ratio of the proportion of carbonaceous material to ferrous material in the proportion of 10% to 90% and the maximum particle size of both materials equal to 4 mm.

When pressing a mixture consisting of a single component, the compressibility increases indefinitely with a simultaneous decrease in the hardness of mineral particles and an increase in the binder content. It has also been found that the dynamic viscosity of the liquid binder has practically no effect on the compressibility of the charge.

Mathematical models and generalized recommendations, made based on their analysis, can be used in the development of briquetting technologies to achieve the required density of the agglomerated product. The paper also proposes a classification of compressibility factors, which made it possible to identify promising areas for further research on the process of compression of the metallurgical charges.

CRediT authorship contribution statement

Alexander Khudyakov: Conceptualization, Data curation, Formal analysis, Investigation, Methodology, Writing – original draft. **Sergii Vashchenko:** Conceptualization, Data curation. **Kostiantyn Baiul:** Data curation, Investigation, Methodology. **Yurii Semenov:** Methodology, Formal analysis, Writing – review & editing. **Pavlo Krot:** Supervision, Formal analysis, Writing – review & editing.

Declaration of Competing Interest

The authors declare that we have no financial and personal relationships with other people or organizations that can inappropriately influence our work; there is no professional or other personal interest of any nature or kind in any product, service and/or company that could be construed as influencing the position presented in, or the review of, the manuscript.

Data availability

Data will be made available on request.

References

[1] M. Ehman, L.J. Nilsson, B. Johansson, Global climate policy and deep decarbonization of energy-intensive industries, Clim. Pol. 17 (5) (2017) 634–649, https://doi.org/10.1080/14693062.2016.1167009.

[2] J. Rissman, C. Bataille, E. Masanet, et al., Technologies and policies to decarbonize global industry, Appl. Energy 226 (2020), https://doi.org/10.1016/j.apenergy.2020.114848. Article 114848.

[3] Paris Agreement to the United Nations Framework Convention on Climate Change, Dec. 12, 2015. T.I.A.S. No. 16–1104.

[4] A. Nurdiawati, F. Urban, Towards deep decarbonisation of energy-intensive industries: a review of current status, technologies and policies, Energies 14 (2021), https://doi.org/10.3390/en14092408. Article 2408.

[5] S.K. Dutta, Y.B. Chokshi, Basic Concepts of iron and Steel Making, Springer Nature, Singapore, 2020, p. 645, https://doi.org/10.1007/978-981-15-2437-0.

[6] Y. Junjie, Progress and future of breakthrough low-carbon steelmaking technology of EU, Int. J. Miner. Process. Extract. Metallur. 3 (2) (2018) 15–22, https://doi.org/10.11648/j.ijmpem.20180302.11.

[7] Y. Chan, L. Petithuguenin, T. Fleiter, et al., Industrial innovation: pathways to deep decarbonisation of industry. Part 1: technology analysis, in: Report Submitted by ICF Consulting Services and Fraunhofer ISI to the European Commission, ICF, London, UK, 2019, p. 124.

[8] M. Saha, Reduction in charge requirements of HIsmelt iron-making process in Indian context, Am. J. Eng. Res. 6 (12) (2017) 102–108.

[9] J. Van der Stel, K. Meijer, Ch. Zeilstra, et al., HIsarna smelting reduction. A solution for sustainable hot metal production, in: International Conference. Zaandam and Petten, Netherlands, CATO-ECN, 19-20 April, 2017, p. 24.

[10] R. Bechara, H. Hamadeh, O. Mirgaux, et al., Carbon impact mitigation of the iron ore direct reduction process through computer-aided optimization and design changes, Metals 10 (2020), https://doi.org/10.3390/met10030367. Article 367.

[11] M.M. Ahmed, M.A. Shahin, M.A. Elzeky, et al., Effect of HYL process parameters on the quality of iron ore reduction, J. Petrol. Min. Eng. 18 (1) (2016) 54–60, https://doi.org/10.21608/JPME.2016.37810.

[12] M. Pei, M. Petajaniemi, A. Regnell, et al., Toward a fossil free future with HYBRIT: development of iron and steelmaking technology in Sweden and Finland, Metals 10 (2020), https://doi.org/10.3390/met10070972. Article 972.

[13] M. Barberousse, M. Apostolou, A. Debregeas, et al., Electrification of primary steel production based on SIDERWIN process simulation on the European power system in 2050, ECEEE Indus. Summer Study Proc. 6 (063) (2020) 435–443.

[14] A. Keys, M. Van Hout, B. Daniels, Decarbonisation Options for the Dutch Steel Industry. Joint Publication by PBL Netherlands Environmental Assessment Agency and ECN Part of TNO, PBL&ECN, Hague, Netherlands, 16 September 2021, p. 66.

[15] V. Vogl, O. Olsson, B. Nykvist, Phasing out the blast furnace to meet global climate targets, Joule 5 (10) (2021) 2646–2662, https://doi.org/10.1016/j.joule.2021.09.007.

[16] M. Geerdes, H. Toxopeus, G. Calis, On the future of blast furnace ironmaking, in: 8th Ironmaking Conference, Rosario, Argentina, IAS, 2011, p. 8.

[17] M. Geerdes, R. Chaigneau, O. Lingiardi, et al., Modern Blast Furnace Ironmaking: An Introduction, IOS Press, Amsterdam, 2020, p. 274.

[18] K. Baiul, A. Khudyakov, S. Vashchenko, et al., The experimental study of compression parameters and elastic after-effect of fine fraction raw materials, Min. Sci. 27 (2020) 7–18, https://doi.org/10.37190/msc202701.

[19] K. Baiul, S. Vashchenko, A. Khudyakov, et al., Optimization of wastes compaction parameters in case of gradual wear of the briquetting press rolls, in: G. Lesiuk, M. Szata, W. Blazejewski, A.M.d. Jesus, J.A. Correia (Eds.), Structural Integrity and Fatigue Failure Analysis. VCMF 2020. Structural Integrity 25, Springer, Cham, 2022, pp. 293–302, https://doi.org/10.1007/978-3-030-91847-7_27.

[20] K. Baiul, N. Solodka, A. Khudyakov, et al., Selection of rational surface configuration for roller press tires, Powder Metallur. Metal Ceram. 59 (1–2) (2020) 9–21, https://doi.org/10.1007/s11106-020-00133-w.

[21] S.V. Vashchenko, A.Yu. Khudyakov, K.V. Baiul, Yu.S. Semenov, Method for predicting the strength of pellets produced from dry fine-grained materials, Powder Metallur. Metal Ceram. 60 (3–4) (2021) 247–256, https://doi.org/10.1007/s11106-021-00233-1.

[22] M. Bembenek, A. Uhrynski, Analysis of the temperature distribution on the surface of saddle-shaped briquettes consolidated in the roller press, Materials 14 (7) (2021), https://doi.org/10.3390/ma14071770. Article 1770.

[23] M. Bembenek, A. Zieba, M. Kopyscianski, et al., Analysis of the impact of the consolidated material on the morphology of briquettes produced in a roller press, J. Mater. Eng. Perform. 29 (6) (2020) 3792–3799, https://doi.org/10.1007/s11665-020-04898-4.

[24] F. Su, H. Lampinen, R. Robinson, Recycling of sludge and dust to the BOF converter by cold bonded pelletizing, ISIJ Int. 44 (4) (2004) 770–776, https://doi.org/10.2355/isijinternational.44.770.

[25] I.F. Kurunov, O.G. Bolshakova, Briquets for washing blast furnaces, Metallurgist 51 (5–6) (2007) 253–261, https://doi.org/10.1007/s11015-007-0048-7.

[26] I.F. Kurunov, T.Ya. Malysheva, Bol'shakova O.G., A study of the phase composition of iron-ore briquettes to assess their behavior in a blast furnace, Metallurgist 51 (9–10) (2007) 548–557, https://doi.org/10.1007/s11015-007-0101-6.

[27] A. Bizhanov, V. Chizhikova, Agglomeration in Metallurgy, Springer International Publishing, Cham, 2020, p. 454.

[28] I. Kurunov, A. Bizhanov, Stiff Extrusion Briquetting in Metallurgy, Springer, 2017, 169 p.

[29] Yu.S. Semenov, V.V. Horupakha, M.A. Alter, S.V. Vashchenko, A.Yu. Khudyakov, E.I. Shumelchik, Efficiency of washing blast furnace hearth in case of Pulverized coal injection, in: Proceedings of the Iron & Steel Technology Conf. AISTech 2022, 16–18 May 2022, Pittsburgh, PA, USA, 2022, pp. 219–230, https://doi.org/10.33313/386/025.

[30] A. Babich, D. Senk, H.W. Gudenau, et al., Ironmaking, RWTH Aachen University, Aachen, 2008, p. 402.

[31] A.K. Biswas, Principles of Blast Furnace Ironmaking, SBA Publication, Calcutta, 1981, p. 528.

[32] V. Penkavova, L. Kulaviak, M.C. Ruzicka, et al., Compression of anisometric granular materials, Powder Technol. 342 (2019) 887–898, https://doi.org/10.1016/j.powtec.2018.10.031.

[33] R. Panelli, F. Ambrozio Filho, A study of a new phenomenological compacting equation, Powder Technol. 114 (1–3) (2001) 255–261, https://doi.org/10.1016/S0032-5910(00)00207-2.

[34] O. Arndt, P. Kleinebudde, Influence of binder properties on dry granules and tablets, Powder Technol. 337 (2018) 68–77, https://doi.org/10.1016/j.powtec.2017.04.054.

[35] L. Perez-Gandarillas, A. Mazor, D. Souriou, et al., Compaction behavior of dry granulated binary mixtures 285, 2015, pp. 62–67, https://doi.org/10.1016/j.powtec.2015.05.003.
[36] P. Prusti, K. Barik, N. Dash, et al., Effect of limestone and dolomite flux on the quality of pellets using high LOI iron ore, Powder Technol. 379 (2021) 154–164, https://doi.org/10.1016/j.powtec.2020.10.063.
[37] P. Garcia-Trinanes, M. Morgeneyer, J.J. Casares, et al., Use of organic byproducts as binders in the roll compaction of caustic magnesia, Powder Technol. 226 (2012) 173–179, https://doi.org/10.1016/j.powtec.2012.04.039.
[38] K.V. Probst, K.E. Ileleji, The effect of process variables on drum granulation behavior and granules of wet distillers grains with solubles, Adv. Powder Technol. 27 (4) (2016) 1347–1359, https://doi.org/10.1016/j.apt.2016.04.029.
[39] S. Patra, V. Rayasam, Pelletization of iron ore fines with parameter optimization through Box-Benken design, Mater. Sci. Eng. Int. J. 2 (6) (2018) 287–292, https://doi.org/10.15406/mseij.2018.02.00072.
[40] N.A. Babailov, L.I. Polyanskii, Y.N. Loginov, Briquetting metallurgical lime screenings and parameters making it possible to improve process efficiency, Metallurgist 60 (2016) 576–580, https://doi.org/10.1007/s11015-016-0334-3.
[41] M. Ordiales, J. Iglesias, D. Fernandez-Gonzalez, et al., Cold agglomeration of ultrafine oxidized dust from ferromanganese and silicomnganese industrial process, Metals 6 (2016), https://doi.org/10.3390/met6090203. Article 203.
[42] A.Yu. Khudyakov, S.V. Vashchenko, K.V. Baiul, et al., Kaolin raw material briquetting for lump chamotte production, Refract. Ind. Ceram. 59 (4) (2018) 333–337, https://doi.org/10.1007/s11148-018-0231-3.
[43] S.K. Dutta, Iron ore-coal composite pellets and briquettes as new feed material for iron and steelmaking. Material science and engineering, Int. J. 1 (1) (2017), https://doi.org/10.15406/mseij.2017.01.00003. Article 00003.
[44] S.Y. Narita, M.B. Mourao, C. Takano, Development of composite briquettes of iron ore and coal hardened by heat treatment, Ironmak. Steelmak. 42 (7) (2015) 548–552, https://doi.org/10.1179/1743281214Y.0000000260.
[45] A.N. Korchevski, N.A. Zviagintseva, Experimental study of briquetting technology for iron-bearing metallurgical waste treatment, Min. Inform. Anal. Bull. 9 (2019) 122–130, https://doi.org/10.25018/0236-1493-2019-09-0-122-130.
[46] A.Yu. Khudyakov, S.V. Vashchenko, K.V. Baiul, Yu.S. Semenov, Experimental verification of new compression equations for fine materials of the mining and metallurgical complex. Part 1. Basic compression equation, Refract. Ind. Ceram. 62 (1) (2021) 15–24, https://doi.org/10.1007/s11148-021-00554-z.
[47] R.M. German, Powder Metallurgy and Particulate Materials Processing, Metal Powder Industries Federation, Princeton, NJ, USA, 2005, p. 528.
[48] B. Li, S.P. Baker, et al., Advances in Powder and Ceramic Materials Science, Springer International Publishing, Cham, 2020, p. 162.
[49] I.N. Popescu, R. Vidu, Compression behavior modelling of metal-ceramic powder mixtures, Sci. Bull. Valahia Univ. Mater. Mech. 16 (14) (2018) 28–37, https://doi.org/10.1515/bsmm-2018-0006.
[50] J. Bao, M. Chu, H. Wang, et al., Evolution characteristics and influence mechanism of binder addition on metallurgical properties of iron carbon agglomerates, Metall. Mater. Trans. B Process Metall. Mater. Process. Sci. 51 (6) (2020) 2785–2796, https://doi.org/10.1007/s11663-020-01962-1.
[51] D. Mombelli, D.L. Goncalves, C. Mapelli, et al., Processing and characterization of self-redusing briquettes made of jarosite and blast furnace sludges, J. Sustain. Metallur. 7 (4) (2021) 1603–1626, https://doi.org/10.1007/s40831-021-00419-2.
[52] G.W. Oehlert, A First Course in Design and Analysis of Experiments, University of Minnesota, Minneapolis, 2010, p. 679.
[53] A. Dean, M. Morris, J. Stufken, et al., Handbook of Design and Analysis of Experiments, Tailor and Francis Group, Boca Raton, 2016, p. 946.
[54] A.I. Lurie, A. Belyaev, Theory of Elasticity, Springer, Berlin, Heidelberg, 2005, https://doi.org/10.1007/978-3-540-26455-2, 1050 p.
[55] H. Masuda, K. Higashitani, H. Yoshida, Powder Technology Handbook, Tailor and Francis Group, Boca Raton, 2006, 878 p.
[56] J. Loveday, High-Pressure Physics, Chapman and Hall/CRC, London, 2016, p. 342.
[57] Khudyakov A. Yu, S.V. Vashchenko, Analysis of known dependencies and construction of new compression equations for fine materials of the mining and metallurgical complex, Refract. Ind. Ceram. 60 (6) (2020) 618–626, https://doi.org/10.1007/s11148-020-00417-z.
[58] N.V. Andreeva, I.D. Radomysel'skii, N.I. Sherban, Compressibility of powders, Powder Metallur. Metal Ceram. 14 (6) (1975) 457–464, https://doi.org/10.1007/BF00823503.
[59] A.Yu. Khudyakov, S.V. Vashchenko, K.V. Baiul, et al., New method for predicting the compressibility of charges made from fine materials of the mining and smelting industry, Metallurgist 65 (9–10) (2022) 941–951, https://doi.org/10.1007/s11015-022-01234 0.
[60] ISO 3927:2017, Metallic powders, excluding powders for hard metals. Determination of compressibility in uniaxial compression, ISO Copyright Office, Geneva, Switzerland, 2017, 9 p.
[61] S.V. Vashchenko, Development of Scientific Bases for the Production of Raw Materials for the Metallurgical Industry by Briquetting (in Russian), PhD thesis., Iron and Steel Institute of Z.I. Nekrasov NAS of Ukraine, 2014.
[62] D.P. Bertsekas, Constrained Optimization and Lagrange Multiplier Methods, Athena Scientific, Belmont, Massachusetts, 1996, p. 410.
[63] L. Kieush, A. Koveria, M. Boyko, et al., Walnut shells as a potential fuel for Iron ore sintering, Mater. Sci. Forum 1045 (2021) 127–140, https://doi.org/10.4028/www.scientific.net/MSF.1045.127.
[64] L. Kieush, A. Koveria, Z. Zhu, et al., Application of biomass pellets for Iron ore sintering, Mater. Sci. Forum 1045 (2021) 17–31, https://doi.org/10.4028/www.scientific.net/MSF.1045.17.
[65] V.V. Zuev, Concept of core electron structure of minerals, Gornyi Zhurnal 5 (2015) 23–29, https://doi.org/10.17580/gzh.2015.05.05.
[66] H.J.H. Brouwers, Packing fraction of geometric random packings of discretely sized particles, Phys. Rev. E 84 (2011), https://doi.org/10.1103/PhysRevE.84.042301. Article 042301.
[67] O. Koutny, J. Kratochvil, J. Svec, et al., Modeling of packing density for particle composites design, Proc. Eng. 151 (2016) 198–205, https://doi.org/10.1016/j.proeng.2016.07.386.
[68] L. Burtseva, B.V. Salas, R. Romero, et al., Multi-Sized Sphere Packings: Models and Recent Approaches, Preprint 02/15,, Faculty of Mathematics, Otto-von-Guericke-Universität Magdeburg, Germany, January 2015, https://doi.org/10.13140/2.1.4515.6169, 21 p.